TU Delft

Delft University of Technology

The potential of air micro-nano bubbles and nucleated CO2 bubbles as curative and preventive strategies for SWRO biofouling removal

Alvarez Sosa, Damaris S.; Alpatova, Alla; Ybyraiymkul, Doskhan; Ng, Kim Choon; Ghaffour, Noreddine; Vrouwenvelder, Johannes S.; Farhat, Nadia

DOI
10.1016/j.desal.2025.118865

Publication date
2025

Document Version
Final published version

Published in
Desalination

Citation (APA)
Alvarez Sosa, D. S., Alpatova, A., Ybyraiymkul, D., Ng, K. C., Ghaffour, N., Vrouwenvelder, J. S., & Farhat, N. (2025). The potential of air micro-nano bubbles and nucleated CO2 bubbles as curative and preventive strategies for SWRO biofouling removal. *Desalination*, *610*, Article 118865. https://doi.org/10.1016/j.desal.2025.118865

Important note
To cite this publication, please use the final published version (if applicable).
Please check the document version above.

Copyright
Other than for strictly personal use, it is not permitted to download, forward or distribute the text or part of it, without the consent of the author(s) and/or copyright holder(s), unless the work is under an open content license such as Creative Commons.

Takedown policy
Please contact us and provide details if you believe this document breaches copyrights.
We will remove access to the work immediately and investigate your claim.

This work is downloaded from Delft University of Technology.
For technical reasons the number of authors shown on this cover page is limited to a maximum of 10.

Green Open Access added to TU Delft Institutional Repository

'You share, we take care!' - Taverne project

https://www.openaccess.nl/en/you-share-we-take-care

Otherwise as indicated in the copyright section: the publisher is the copyright holder of this work and the author uses the Dutch legislation to make this work public.

Desalination 610 (2025) 118865

Contents lists available at ScienceDirect

Desalination

journal homepage: www.elsevier.com/locate/desal

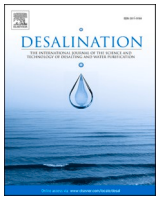

The potential of air micro-nano bubbles and nucleated CO_2 bubbles as curative and preventive strategies for SWRO biofouling removal

Damaris S. Alvarez Sosa [a,*], Alla Alpatova [a], Doskhan Ybyraiymkul [a], Kim Choon Ng [a], Noreddine Ghaffour [a], Johannes S. Vrouwenvelder [a,b], Nadia Farhat [a]

[a] Environmental Science and Engineering Program, Biological and Environmental Science & Engineering (BESE) Division, King Abdullah University of Science and Technology (KAUST), Thuwal 23955-6900, Saudi Arabia
[b] Department of Biotechnology, Faculty of Applied Sciences, Delft University of Technology, Van der Maasweg 9, HZ, Delft 2629, the Netherlands

HIGHLIGHTS

- MNBs and nucleated CO_2 bubbles treatments showed a clear biofilm reduction; enhanced for seawater environments.
- Daily preventive micro-nano bubble and nucleated CO_2 bubble treatments extended the membrane performance.
- Daily biofilm exposure to micro-nano bubbles and nucleated CO_2 bubbles enhanced extracellular polymeric substances.

GRAPHICAL ABSTRACT

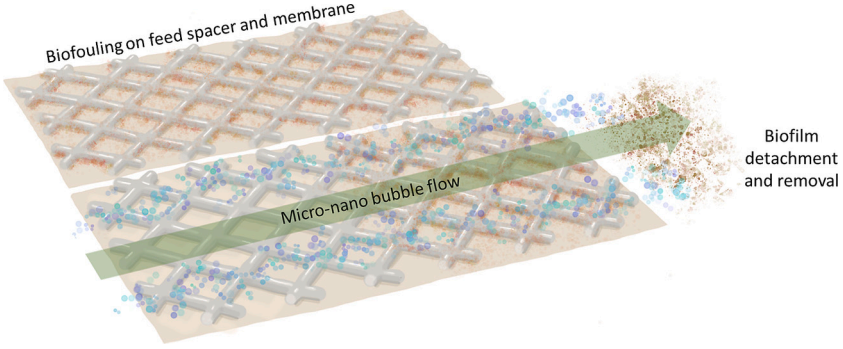

ARTICLE INFO

Keywords:
Reverse osmosis desalination
Membrane autopsy
Micro-nano bubbles
Nucleated CO_2 bubbles
Biofouling
Membrane cleaning
Biofilm removal

ABSTRACT

Seawater reverse osmosis (SWRO) membrane systems face inevitable performance decline due to biofouling, which imposes significant economic costs, accounting up to 25 % of water production costs in desalination plants. Current industry practices primarily rely on chemical cleaning treatments to restore membrane performance. However, these methods involve substantial expenses related to chemical acquisition, storage, and transportation, extended plant downtimes, and premature membrane replacement due to reduced lifespan. Additionally, the disposal of chemical waste raises serious environmental concerns. Micro-nano bubbles (MNBs), consisting of gas-filled cavities (from <1 μm to 5 μm in diameter), have emerged as a promising alternative for biofouling control. This study evaluates the performance of the air-filled (AMNBs) and CO_2-nucleated bubbles (N_CO_2) as curative cleaning-in-place (CIP) treatments and preventive daily treatments under conditions representative of SWRO systems. Using membrane fouling simulators (MFSs) and pressure drop as a performance indicator, curative AMNBs, and N_CO_2 treatments achieved 49 %–56 % pressure drop recovery, comparable to conventional chemical cleaning (51 %) and significantly outperforming hydraulic flushing (24 %). Optical coherence tomography (OCT) imaging and biomass analyses confirmed these findings, revealing effective biofilm removal due to MNB's action. Preventive treatments demonstrated that Nucleated CO_2 bubbles delayed performance decline by 123 %, AMNBs by 95 %, and hydraulic flushing by only 15 % compared to controls. OCT

* Corresponding author.
E-mail address: damaris.alvarezsosa@kaust.edu.sa (D.S. Alvarez Sosa).

https://doi.org/10.1016/j.desal.2025.118865
Received 2 February 2025; Received in revised form 25 March 2025; Accepted 2 April 2025
Available online 3 April 2025
0011-9164/© 2025 Elsevier B.V. All rights are reserved, including those for text and data mining, AI training, and similar technologies.

imaging and membrane biomass analysis confirmed reduced biofilm growth and biomass accumulation in bubble-treated systems. These results indicate that MNB technologies hold great potential as a sustainable and eco-friendly alternative to chemical cleaning for biofouling management in SWRO systems.

1. Introduction

Seawater desalination is an essential solution for securing freshwater supplies, particularly in arid and semi-arid regions. Among desalination technologies, seawater reverse osmosis (SWRO) accounts for 65 % of global desalinated water capacity [1]. However, SWRO membranes are highly susceptible to fouling, where accumulated suspended solids degrade system performance. Fouling originates from various sources, including particulate matter [2], inorganic scaling [3], organic compounds [4], and biofouling [5], often occurring simultaneously and influencing each other [6]. While inorganic scaling is controlled through chemical dosing, and particulate fouling is mitigated via pre-treatment (e.g., ultrafiltration), biofouling—caused by excessive bacterial growth—remains the most challenging issue in SWRO plants due to its severe impact on membrane performance and associated operational costs [7].

Current biofouling control relies heavily on membrane cleaning, classified into physical and chemical methods. Physical techniques, such as backflushing, air sparging, and sonication, leverage mechanical or hydraulic forces to dislodge biofilms [8]. Chemical cleaning, in contrast, employs alkaline or acidic solutions, chelating agents, and surfactants to dissolve biofouling deposits [9]. However, these methods present significant drawbacks. Physical cleaning alone is often insufficient, while chemical treatments pose environmental concerns, require costly chemicals, and risk membrane degradation, leading to extended downtimes [10,11]. Moreover, studies indicate that chemical cleaning may inadvertently exacerbate biofouling by altering membrane surface properties or leaving residual nutrients that promote bacterial regrowth [12,13]. These limitations underscore the need for innovative, sustainable, and effective biofilm removal strategies.

Micro-nano bubbles (MNBs) have emerged as a promising membrane cleaning technology due to their unique physicochemical properties. Unlike conventional gas bubbles that quickly rise and burst, MNBs behave differently based on size. Microbubbles (1–100 μm) ascend slowly, extending their retention time in the liquid, while nanobubbles (<1 μm) remain suspended in solution due to Brownian motion, maintaining stability for extended periods [14–16]. Their cleaning potential stems from their ability to penetrate biofilm structures. As microbubbles collapse, they generate expansive shock waves and localized heating, facilitating biofilm detachment [17]. Agarwal et al. [18,19] demonstrated that microbubbles significantly (>80 %) reduced biomass and extracellular polymeric substances (EPS) on nylon membranes when applied to synthetic wastewater biofilms. Nanobubbles, by contrast, induce turbulence through repulsive forces, further enhancing foulant removal [20,21].

Multiple approaches exist for MNB generation, with hydrodynamic cavitation and gas nucleation emerging as effective methods [22–25]. Hydrodynamic cavitation occurs when rapid pressure variations induce vaporization, forming bubbles within a flowing liquid, as seen in Venturi-based systems [26]. Other cavitation mechanisms include mechanical agitation [27], flow constriction [28], and axial flow shearing [29]. Gas nucleation, particularly for CO_2, occurs when a supersaturated CO_2 solution experiences a phase change, leading to bubble formation [30]. This method has shown promise in enhancing biofilm and scaling removal in RO membranes during rinsing [31] and backwashing for ultrafiltration systems [32–34]. The generated bubbles exert hydrodynamic forces that facilitate foulant detachment [34]. Notably, Ngene et al. [31] successfully removed biofouling from RO membranes using CO_2 nucleation bubbles in a recirculating system, while Alnajjar et al. [30] demonstrated effective organic fouling removal at pressures of 2–6 bar. Additional applications of CO_2 nucleation for membrane cleaning are summarized in Supplementary Table 2.

While MNBs and CO_2 nucleation have been explored for cleaning organic fouling [35–38], scaling [39], and biofilms formed in synthetic or environmental water matrices [19], key knowledge gaps remain. Previous studies have not investigated biofilm removal in a single-pass SWRO setup with permeation, which better replicates real-world biofouling conditions. Additionally, no direct comparison exists between bubble-based cleaning methods for biofilms developed in both tap water and seawater environments. The aim of this study is to build upon existing research by evaluating the long-term effectiveness of two novel bubble-based physical biofilm removal methods—air-filled micro-nano bubbles (AMNBs) and CO_2 nucleated bubbles (N_CO_2) as cleaning-in-place (CIP) and preventive daily treatments. Using membrane fouling simulators (MFS), we assessed the impact of these methods on biofilm growth delay and biomass removal under operationally relevant conditions to SWRO.

2. Materials and methods

2.1. Experimental setup

A membrane fouling simulator (MFS) serves as a representative of the first 0.20 m of a full RO spiral wound membrane element and was used for accelerated biofilm development studies [40]. The setup was comprised of a feed water pump (Cole-Parmer®, USA), a feed flow controller (Bronkhorst, Ruurlo, Netherlands), a nutrient dosing pump (Bronkhorst, Ruurlo, Netherlands), an MFS, a permeate flow controller (Bronkhorst, Ruurlo, Netherlands), a differential pressure sensor (Delta bar, PMD75, Endress + Hauser, Switzerland), and a back pressure valve (Bronkhorst, Ruurlo, Netherlands) as presented in Supplementary Fig. 1. CORI-FLOW™ meters & controllers monitored the system's feed flow, pressure, nutrient dosing, and permeate flow. These parameters were recorded using a LabVIEW™ interface on a minute basis.

Feed water for all experiments comprised of both tapwater, for curative and preventive experiments and seawater for curative experiments. For the tap water experiments setup, the system was fed with water produced by the King Abdullah University of Science and Technology seawater desalination plant (Thuwal, Jeddah, Saudi Arabia). The feed water passed through a filtering step comprised of two activated carbon filters (Pentair Pentek GAC-20BB, USA) to remove residual chlorine, and a cartridge filter (pore size 10 μm) to remove particles from the feed water. In contrast, for the seawater experiments, seawater was sourced from the Red Sea and passed through a sand filtration pretreatment at the WDRC desalination pilot plant (Thuwal, Jeddah, Saudi Arabia), followed by a 3-filtering unit comprised of one carbon and 2 cartridge sediment filters.

Before every experiment, a full setup cleaning was performed with 2 mL/L of sodium hypochlorite through the main feed line and the nutrient dosing line, followed by a 48-hour MQ (Millipore, USA) water rinse. Membrane (FilmTec™ NF90 Dupont, USA), permeate spacer (FilmTec™ NF90 Dupont, USA), and commercially available 26 mil feed spacers were cut into 7 cm × 27 cm and 4 cm × 20 cm rectangular segments respectively via laser cutter (Epilog Legend Laser Engraver-Mini 24, USA). The active membrane filtration area was 80 cm^2. The membrane, feed, and permeate spacer were assembled into the MFSs and screwed together as shown in Supplementary Fig. 1. The assembled MFSs were connected to their respective setup as shown in Fig. 1.

2.2. Operating conditions and monitoring

The feed water was pumped into the system at a constant flow rate of 20 L/h equivalent to a crossflow velocity of $v_{sp} = 0.22$ m/s. The membranes were left to acclimate at a transmembrane pressure of 2 bar at a permeate flux of 50 mL/h equivalent to $J_{sp} = 6.25$ L/m^{2}h for a week. During the biofilm growth stage, the filtered tapwater was fed to the MFSs at $v_{sp} = 0.22$ m/s and permeate flux was maintained at $J_{sp} = 6.25$ L/m^{2}h (see Table 1). Biofilm growth was accelerated by dosing a nutrient stock solution to the feed water increasing the assimilable organic carbon concentration of the feed water by 100 µg C/L. For this Sodium Acetate ($CH_3COONa.3H_2O$), Sodium Nitrate ($NaNO_3$), and Sodium Phosphate Monobasic ($NaH_2PO_4.2H_2O$) were obtained from Sigma Aldrich (Missouri, USA). Nutrient dosing of 30 mL/h occurred after the previously mentioned acclimation week, the nutrient concentrations for all the experiments in this present work followed a Carbon: Nitrogen: Phosphorous ratio of 100:20:10. Detailed amounts are disclosed in Supplementary Table 3. Additionally, the pH for all nutrient dosing solutions was set at 11 by adding NaOH 1 M for bacterial growth prevention in the substrate dosage bottle.

Biofouling growth on a specific location at the middle of each MFS was monitored daily via Optical coherence tomography (OCT) (GAN610C1, Thorlabs GmbH, Germany) using a central light wavelength of 930 nm. The equipment configuration accounted for a refractive index of 1.33 and an A-scan rate of 36 kHz. Additionally, the noise was flattened for better image quality with an A-scan averaging of 20 and a B-scan averaging of 10. Additional images were taken before and after CIP procedures at the same marked location. All 3D images had a resolution of 499 × 499 × 558 voxels in a field of view of 5.0 mm × 5.0 mm × 1.2 mm. These images were processed and optimized using Matlab® (MathWorks, USA).

2.3. MNB generation and treatments

Two sets of experiments were carried out to evaluate the efficiency of both AMNBs and nucleated CO_2 bubbles as: i) curative CIP treatments and ii) preventive daily treatments for biofouling over long-term studies. Treatment durations were determined based on durations previously implemented in literature (as presented in Supplementary Tables 1 and 2) and per CO_2 saturation tank size limitations.

Table 1
Operating parameters for biofilm growth.

Parameter	Units	Value
Permeate production[a]	L/m^{2}h	6.25
Crossflow velocity	m/s	0.22
Substrate dosage concentration	µg C/L	100

[a] For tapwater set up only.

The air MNBs (AMNBs) were generated in a recirculating setup comprised of an air MNBs generator [41] connected to a high flux pump (DC HOUSE 42-Series Upgrade Water Diaphragm) and an airflow controller. The system was operated 1 h before each treatment to ensure the presence of enough MNBs. The generated bubble solution was pumped (Cole-Parmer®, USA) to the MFS setups and back into the microbubble tank at a continuous flux of 20 L/h. MNBs presence was confirmed by the white-milky color of the solution for microbubbles and by the Tyndall effect for nanobubbles (Supplementary Fig. 4).

Saturated CO_2 solution was prepared following an existing method [32 – 34]. Briefly, a CO_2 gas tank was connected to a pressure vessel with 20 L of MilliQ water. MilliQ was used for CO_2 bubble nucleation since ions disrupt the saturation process by stabilizing the CO_2 bubbles thus decreasing the bubble coalescence rates [38]. Saturation pressures varied from 1 to 2 bar depending on the study performed, 2 bar for curative experiments, and 1 bar for daily preventive studies for optimization purposes. After setting the pressure, the saturation tank was left open for 30 min, then the system was closed and left for 48 h to saturate at the desired pressure. No observable MNBs were perceived in the solution (Supplementary Fig. 5).

The curative CIP studies aimed to evaluate the ability of MNBs to restore the membrane flux and permeability from a matured biofouling

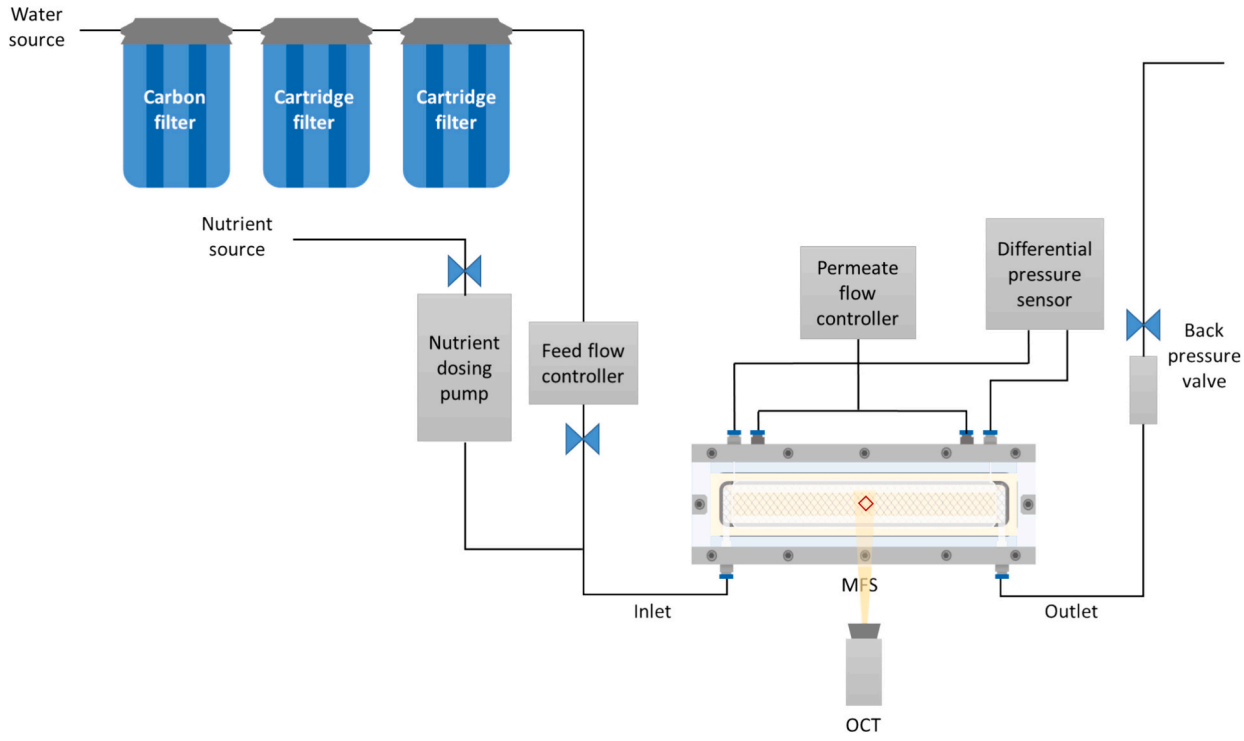

Fig. 1. Membrane fouling simulator (MFS) full setup and components for biofouling growth under tap water and seawater conditions (permeation was only applicable for tap water setup).

layer in conditions like those at a desalination plant. Such studies were carried out for each MNB type in both tap water and seawater setups. Feed channel pressure drop (PD) served as the main performance monitoring parameter as it was shown to be the earliest and strongest impacted parameter by biofilm development [6,42]. CIP was performed once PD reached a 100 % increase, equivalent to the industry-suggested cleaning parameter of 10–15 % [43] in our scaled-down module. Both MNBs treatments AMNBs, and nucleated CO_2 bubbles were compared against conventional physical and chemical cleaning protocols and to a no-cleaning control. Hydraulic flush (HF) served as a physical cleaning control, the conventional chemical cleaning control was comprised of NaOH 0.01 M (pH 12) followed by HCL 0.2 M (pH 1) and an MQ water rinse [44] (see Table 2). Statistical significance was evaluated by a two-sample *t*-test analysis.

In contrast, the preventive studies served to evaluate the ability of MNBs to delay the PD from reaching a 100 % increase on the tap water MFSs setup for which short treatments including a physical treatment control hydraulic flush (HF), preventive AMNBs and preventive saturated CO_2 were performed daily (see Table 3).

2.4. Membrane autopsy and analysis

After each experiment, a membrane autopsy was performed following an existing procedure [44]. Briefly, feed spacer and membrane coupons were cut and added to vials containing MQ water for total organic carbon (TOC), autoclaved tap water for adenosine triphosphate (ATP), and PBS for extracellular polymeric substances (EPS). Then the coupons were mixed and sonicated (Bransonic®1510 Ultrasonic Cleaner, USA) for 5 min.

To quantify active remaining biomass, ATP was measured using the ATP Celsis Luminometer (Advance™, Germany) following the manufacturer's protocol. This equipment measures the amount of light emitted by the enzyme luciferase once it has direct contact with an ATP molecule and thus the amount of light emitted is directly proportional to the amount of ATP in the sample [45], which is measured in relative light units (RLUs).

TOC samples were filtered with a 0.45 μm syringe filter (Tianjin Jinteng experiment equipment, China) and placed in 40 mL glass vials. The carbon present in the accumulated organic matter was analyzed as TOC with a Shimadzu TOC analyzer (TOC-VCPH/CPN, Japan) following the manufacturer's protocol.

EPS was extracted via the formaldehyde-NaOH method [46], based on its high EPS recovery with a low extracellular DNA concentration. Briefly described, 60 μL of formaldehyde 37.6 % (Sigma Aldrich, Germany) was added to each sample and left at 4 °C for 1 h. Then 4 mL of NaOH 1 M was added and left for 3 h at 4 °C. All samples were centrifuged (Sorvall Legend XT Thermo Scientific™, Germany) at 20000 G for 20 min, filtered with a 0.22 μm syringe filter (Millipore Express Millex-GP, Germany), and left to dialyze (Thermofisher SnakeSkin™, USA) in MQ water on a mixer plate at room temperature for 24 h at 400 rpm. Afterward, all samples were collected in 50 mL centrifuge tubes, frozen at −20 °C for 24 h, and freeze-dried (Labconco™, USA) at −50 °C for 48 h. All samples were resuspended in 10 mL MQ. Spectrophotometry was used for EPS detection and quantification. Carbohydrates were quantified using the sulphuric acid-phenol method using a 96-well plate for which H_2SO_4 and phenol 5 % wt. were added alongside the samples in their respective well. The well plate was shaken for 10 min and then incubated at 90 °C for 1 h and 30 min. Absorbance was measured by a Spectra Max-4 spectrophotometer (Molecular Devices, CA) at a wavelength of 490 nm. Total proteins were quantified with a BCA assay kit (Thermo Fisher Scientific, USA) and measured at an absorbance wavelength of 562 nm with the same equipment.

Table 3
Operating conditions for tapwater MNB preventive treatments.

Treatment	pr-HF	pr-AMNBs	pr-N_CO_2
Operation conditions	Raise flux by 100 %	Continuous AMNBs flux	Intermittent CO_2 flux
Duration	10 min	10 min	45 s
Flow rate	40 L/h	20 L/h	30 L/h
Crossflow velocity	0.45 m/s	0.22 m/s	4.34/s

2.5. Filter autopsy and analysis

Dead-end filtering units with 10 μm nylon net 47 mm filters (Merck™, Germany) were placed on the outlet side of the MFS during the seawater CIP treatments to capture and analyze the biomass removed from the membrane surface. Biomass was analyzed in terms of TOC using the protocol mentioned above. Additionally, total cell count (TCC) was measured using flow cytometry following a protocol by [47]. For this, 700 μL of each sample were stained with 7 μL of a 100X SYBR green (obtained from a 10,000X stock solution (Molecular Probes, Eugene, OR, USA), diluted in Tris buffer, pH 8 into opaque 1.5 mL Eppendorf tubes. The solutions were then incubated at 37 °C for 10 min, and then 200 μL of each sample was poured into a 96-well plate. BD Accuri C6 plus flow cytometer (BD Accuri Cytometer, Belgium) was used to perform the measurements at 488 nm for the fluorescence emission detector (FL1 = 533 ± 30 nm) and a volume of 50 μL, measured at a high flow velocity of 66 μL/min. An electronic gate was established according to Hammes & Egli [48]. Data were processed using the BD Accuri CFlow® software. All samples were analyzed in triplicate.

3. Results

Two sets of experiments were carried out to evaluate the efficiency of both AMNBs and CO_2 nucleated MNBs as: i) curative CIP treatments and ii) preventive daily treatments for biofouling over long-term studies.

3.1. Curative studies

3.1.1. Biofilm growth: pressure drop development in time

Biofilm growth inside the membrane fouling simulators (MFS) for all curative CIP experiments was monitored until a 100 % increase in PD was observed for all MFSs. Fig. 2 shows the average relative PD over time for all duplicates.

The desired growth was achieved for both experiments from day 4 onwards. However, some PD fluctuations were observed, especially for the seawater experiments. This can be attributed to variations in the seawater source and minor PD sensor pauses. Regardless, these

Table 2
Operating conditions for MNB curative CIP treatments.

Treatment	AMNBs	N_CO_2	[a]HF	NaOH/HCl
Operation conditions	Continuous AMNBs flux	Continuous Nucleated CO_2 bubbles flux	Raise flux by 100 %	NaOH 0.1 M followed by HCl 0.2 M and an MQ water rinse
Duration	1 h	3 min	1 h	1 h for each 15 min for the MQ rinse
Flow rate	20 L/h	135 L/h	40 L/h	20 L/h
Crossflow velocity	0.22 m/s	1.53 m/s	0.45 m/s	0.22 m/s

[a] For tapwater experiments only.

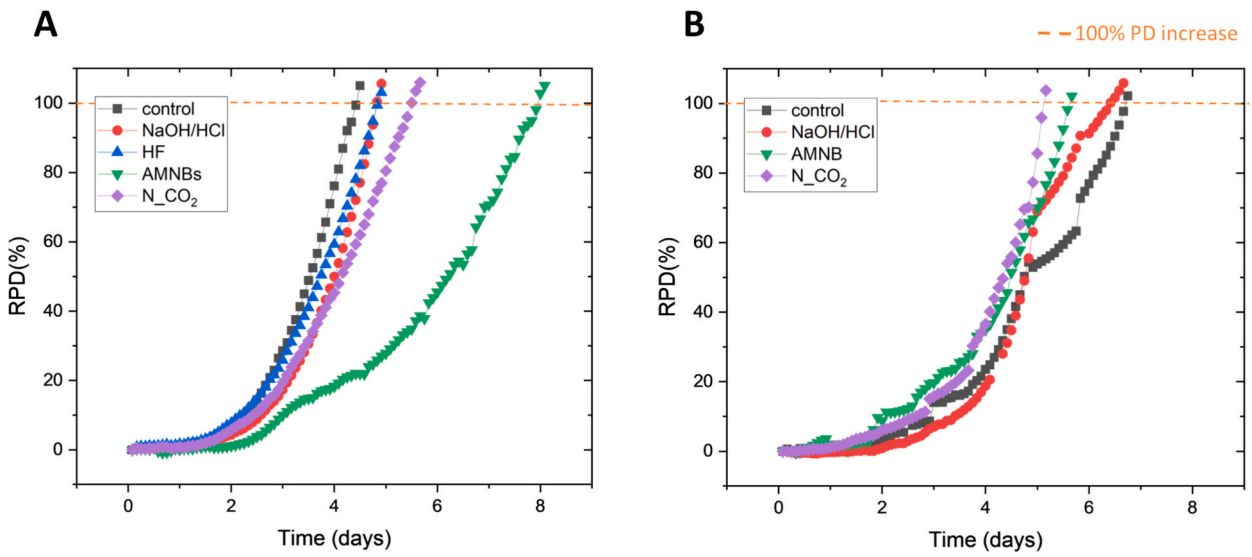

Fig. 2. Relative pressure drop (RPD) development in time from the start of nutrient dosing as day 0 for A) tap water and B) seawater MFS experiments.

fluctuations did not affect the biofilm growth, signaled by the pressure drop increase over time. Overall, the biofilm growth, measured as a relative pressure drop increase (RPD) in time occurred in a similar range for the evaluated treatments.

Fig. 3 presents the cleaning efficiencies per treatment. Cleaning efficiencies under tap water conditions were in a similar range of (~50 %) for all the evaluated treatments except for the hydraulic flush (HF) which was 23.6 %. Interestingly, the cleaning efficiency increased for seawater biofilms in comparison with tap water for all of the evaluated treatments. The Nucleated CO_2 bubbles cleaning efficiency was 77 % on average, higher than the chemical cleaning control (NaOH/HCl) at 63.4 % but the difference is not statistically significant ($P = 0.09$). The higher cleaning efficiency under seawater conditions could be attributed to differences in the composition and structure of seawater and tap water biofilms, as will be shown in the upcoming OCT images.

3.1.2. *Optical coherence tomography (OCT)*

OCT images before the CIP procedure show clear biofilm growth on the feed spacer surface with occasional minimal growth in the membrane surface for the tap water MFS. As presented in Fig. 4, biofilm detachment was confirmed in the after-CIP images for each evaluated CIP treatment. For the tapwater experiments, HF treatments were ineffective (Fig. 4D), as the before and after CIP OCT images were highly similar. In contrast, the rest of the evaluated treatments (NaOH/HCl, AMNBs, N-CO_2) showed clear biomass removal in their corresponding after-CIP images. It is worth noting that this removal effect is more noticeable for seawater experiments due to the elongated structure of the biofilm in comparison to the fluffy structure of tap water biofilm (Fig. 4A, B, and C), this type of structure accounts for less interactions with the base making it more susceptible to detachment by a physical force.

Additional OCT time stamps of the MNBs CIP treatments for seawater conditions are presented in Supplementary Fig. 7 and show the major removal event (MRE), which took place within the 30 s–1-minute mark for the air micro-nano bubbles (AMNBs) and during the first 15 s for the continuous Nucleated CO_2 bubbles flux. There was no significant difference in the images of the MRE and the after-CIP treatment, indicating a possibility for future CIP duration optimization.

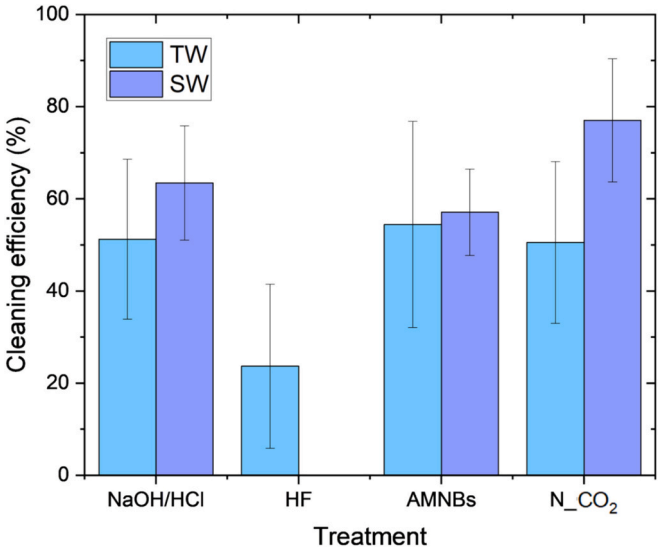

Fig. 3. Cleaning efficiency in terms of relative pressure drop (PD) restoration after cleaning–in–place (CIP) for seawater (SW) and tap water (TW) MFS experiments and their respective standard deviations.

3.1.3. *Membrane autopsy*

Membrane autopsies for both seawater and tap water conditions showed a clear biomass reduction for all of the evaluated treatments in comparison with the no-cleaning control as shown in Fig. 5. For the tap water CIP experiments, the no-cleaning control accounted for an ATP of 86,000 pg/cm^2 and TOC of 15.4 μg/cm^2. The least effective biomass reduction was for the tap water physical cleaning control HF (hydraulic flush) in comparison with the rest of the treatments with an ATP of 48,000 pg/cm^2 and a TOC of 10.7 μg/cm^2. Interestingly, AMNBs showed a similar TOC content at 11.3 μg/cm^2 with a clear ATP reduction at 20,800 pg/cm^2 indicating a possible more effective inactivation with an incomplete biofilm detachment. Nucleated CO_2 bubbles accounted for an ATP of 21,000 pg/cm^2 and TOC of 6.8 μg/cm^2 showing a similar inactivation as AMNBs with better biomass removal. This could be due to the nucleated CO_2 bubbles acting as an additional hydrodynamic shear force. However, none of the evaluated treatments were as effective as the conventional chemical cleaning control at an ATP of 22.4 pg/cm^2 and TOC of 2.9 μg/cm^2.

Of particular relevance, both micro nanobubble treatments AMNBs and Nucleated CO_2 bubbles biomass concentrations under seawater conditions at an ATP of 1899 pg/cm^2 and 188 pg/cm^2 respectively, and TOC values of 8.2 μg/cm^2 and 10.3 μg/cm^2, were closer to the values of the chemical cleaning control (NaOH/HCl) with ATP 90.8 pg/cm^2 of and

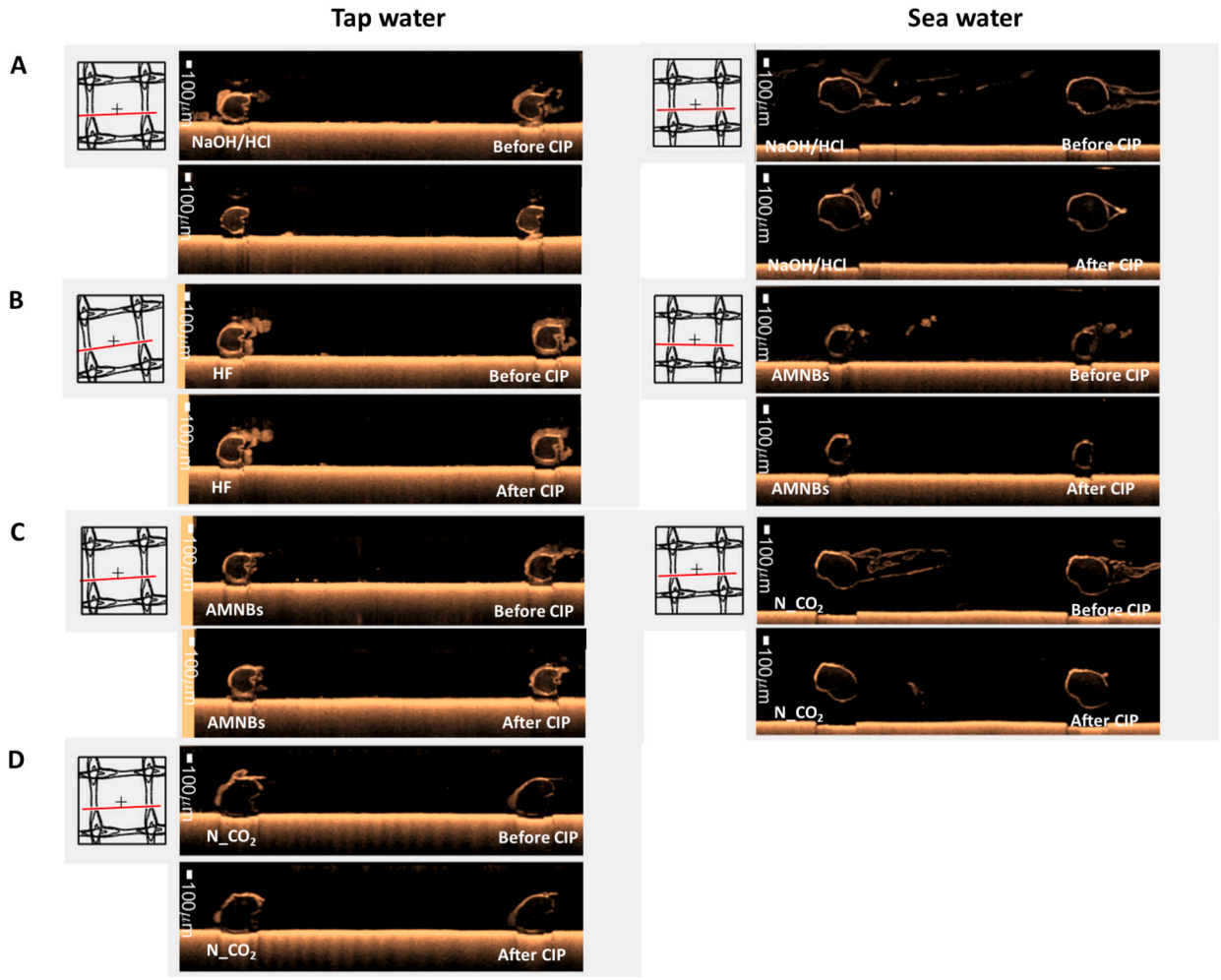

Fig. 4. Optical coherence tomography (OCT) images before and after cleaning-in-place (CIP) for seawater and tapwater environments for A) NaOH/HCl, B) AMNBs, C) Nucleated CO_2 bubbles and D) HF.

TOC of 10.4 μg/cm^2. Considering that the no CIP control biomass accounted for an ATP of 24,500 pg/cm^2 and TOC of 17.2 μg/cm^2, this indicates a better biomass inactivation and removal efficiency for both bubbles treatments in the seawater environment in which nucleated CO_2 bubbles accounted for a similar biomass inactivation and removal capacity as the conventional chemical cleaning control.

3.1.4. *Cleaning in place (CIP) filter autopsy*

Filters were placed on the outlet side of the MFS during seawater CIP treatments to analyze and characterize the biomass removed from the membrane surface. The CIP outlet filter autopsies (Fig. 6) showed either similar or higher biomass values for both of the MNBs treatments (f-AMNBs and f-N_CO_2) in comparison with the chemical cleaning control (f-NaOH/HCl) for TOC indicating a successful biomass removal from the membrane surface and feed spacer. For which the AMNBs accounted for the highest TOC and TCC content at 17.6 μg/cm^2 and 63,100 cells/cm^2 respectively. Indicating that AMNBs showed a higher overall removal of biomass. Additionally, the Nucleated CO_2 bubbles accounted for a similar TOC and higher TCC in comparison with the chemical control at 7.6 μg/cm^2 and 8.0 μg/cm^2 and 44,800 cells/cm^2 and 22,600 cells/cm^2 respectively.

Overall, both types of MNBs showed potential as cleaning strategies for SWRO biofouling. However, Nucleated CO_2 bubbles presented consistent operational cleaning efficiencies and autopsy biofilm removals that were either similar or higher than the conventional chemical control with the advantage that the Nucleated CO_2 bubbles CIP had a duration of 3 min in comparison to the 2 h of the chemical cleaning.

3.2. *Preventive experiments*

3.2.1. *Biofilm growth: pressure drop development in time*

Daily shorter MNBs treatments (pr-AMNBs & pr-N_CO_2) were evaluated against a physical hydraulic flush (pr-HF) control to evaluate their ability to prevent/delay biofilm growth. Fig. 7 shows that both of the MNB treatments effectively delayed the pressure drop from reaching a 100 % increase by an average of 4.5 days. In comparison, the hydraulic flush preventive treatments (pr-HF) delayed the PD (100 % increase) by <1 day. As shown in Fig. 6A), each of the daily preventive treatments resulted in an immediate PD reduction that is reflected in the peaks in the RPD and thus is not present in the controls. Fig. 7B shows the average extended membrane performance before reaching a 100 % PD increase for each preventive treatment compared to the duration of control treatment for which the preventive hydraulic flush (pr-HF) managed to only extend the membrane performance by 15 %. In contrast, both daily bubble preventive treatments roughly doubled the membrane stable operating time with an extended performance of 95 % for preventive AMNBs (pr-AMNBs) and 123 % for preventive Nucleated CO_2 bubbles (pr-N_ CO_2 bubbles). Supplementary Fig. 8 shows the time to reach 100 % PD increase as 8.2 days for pr_AMNBs and 9.3 days for the pr-N_CO_2, in contrast to the 4.2 days for the no-treatment control and the 4.8 days for the pr_HF control.

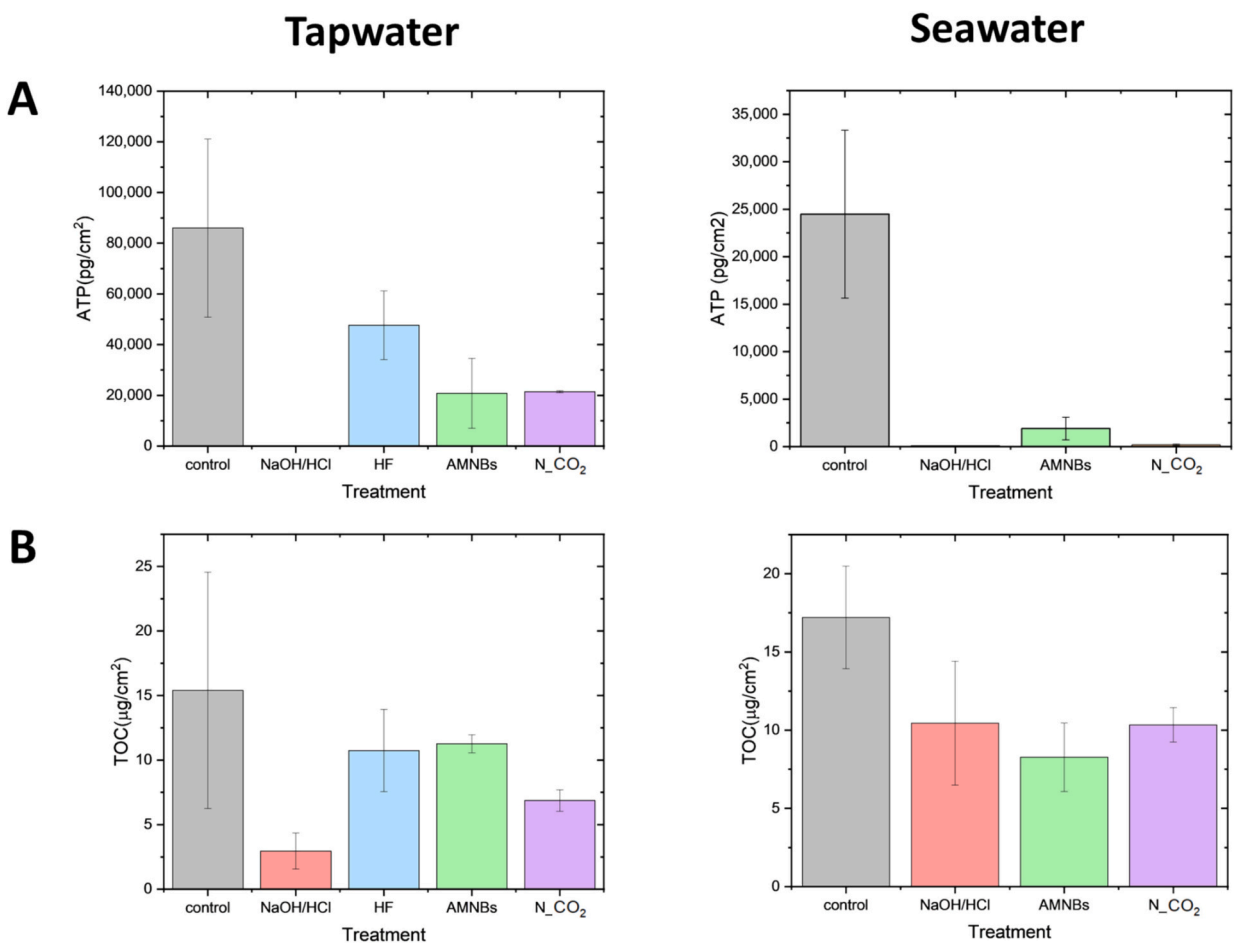

Fig. 5. Biomass quantification on the membrane and spacer after cleaning in place (CIP) quantified as A) adenosine triphosphate (ATP) and B) total organic carbon (TOC) in seawater and tap water MFS experiments.

3.2.2. *Optical coherence tomography (OCT)*

Daily optical coherence tomography (OCT) images from day 4 were selected as a growth control surveillance margin since it accounts for the day when both controls (no treatment and pr-HF) reached a 100 % PD increase and are presented in Fig. 8. At this timeframe, both the control and the HF preventive treatments (pr-HF) showed clear biofilm growth around the feed spacer in addition to some growth on top of the membrane surface. Meanwhile, both preventive MNB treatments (pr-AMNBs and pr-N_CO_2) show minimal biofilm growth surrounding the feed spacer.

3.2.3. *Membrane autopsy*

Membrane autopsies for preventive studies on tap water conditions were performed once each MFS reached a 100 % PD increase, shown in Fig. 9. Nucleated CO_2 bubbles preventive treatments (pr-N_CO_2) accounted for the lowest ATP counts at 55,600 pg/cm^2 indicating lower viable cells present which could explain the extended membrane lifespan of the Nucleated CO_2 bubbles pretreatments in comparison with the other preventive treatments with 101,700 pg/cm^2 for AMNBs (pr-AMNBs) and 92,329 pg/cm^2 for the hydraulic flush (pr-HF). Furthermore, both preventive bubble treatments showed lower TOC values than the hydraulic flushing control (pr_HF) at 11.8 µg/cm^2 and the no treatment control at 8.9 µg/cm^2, with AMNBs (pr-AMNBs) accounting for the lowest TOC at 7.3 µg/cm^2 (statistically significant $P = 0.049$). The Nucleated CO_2 bubbles accounted for slightly higher TOC than the no-treatment control at 9.7 µg/cm^2, likely related to its prolonged duration in comparison to the rest of the treatments. This could be related to a higher EPS composition than the bacterial cell content.

To better understand the effects of constant short-term exposure to MNBs an gas nucleated bubbles on the biofilm composition, extracellular polymeric substances (EPS) were extracted and quantified as shown in Fig. 10. The preventive AMNB treatments accounted for the highest concentration of both EPS proteins and carbohydrates at 145 and 143 µg/cm^2 respectively. This could be attributed to an effect on the biofilm structure or an incomplete removal and further reattachment on the membrane and feed spacer surface. Furthermore, the Nucleated CO_2 bubbles preventive treatments showed slightly higher EPS protein and carbohydrate values at 94 and 78 µg/cm^2 respectively in comparison to the no-treatment control (105 and 73 µg/cm^2) and the HF preventive treatment (95 and 69 µg/cm^2) while being the treatment that resulted in a longer membrane lifespan. These slightly higher EPS concentrations could entail that the preventive treatments could have promoted EPS production but at a significantly lower rate than the AMNB treatments.

Both of the daily preventive MNB treatments were able to extend the membrane lifespan in terms of PD and OCT images with Nucleated CO_2 bubbles resulting in better cell inactivation and AMNBs showing overall lower TOC content. However, an increase in EPS production was perceived and it was more aggravated by AMNBs.

4. Discussion

This study aimed to test the efficiency of both AMNBs and CO_2 nucleated bubbles as (i) cleaning-in-place (CIP) treatments and (ii) preventive daily treatments for biofouling over long-term studies. In addition, their impact on membrane performance and biomass activity was monitored in conditions that simulate a reverse osmosis membrane

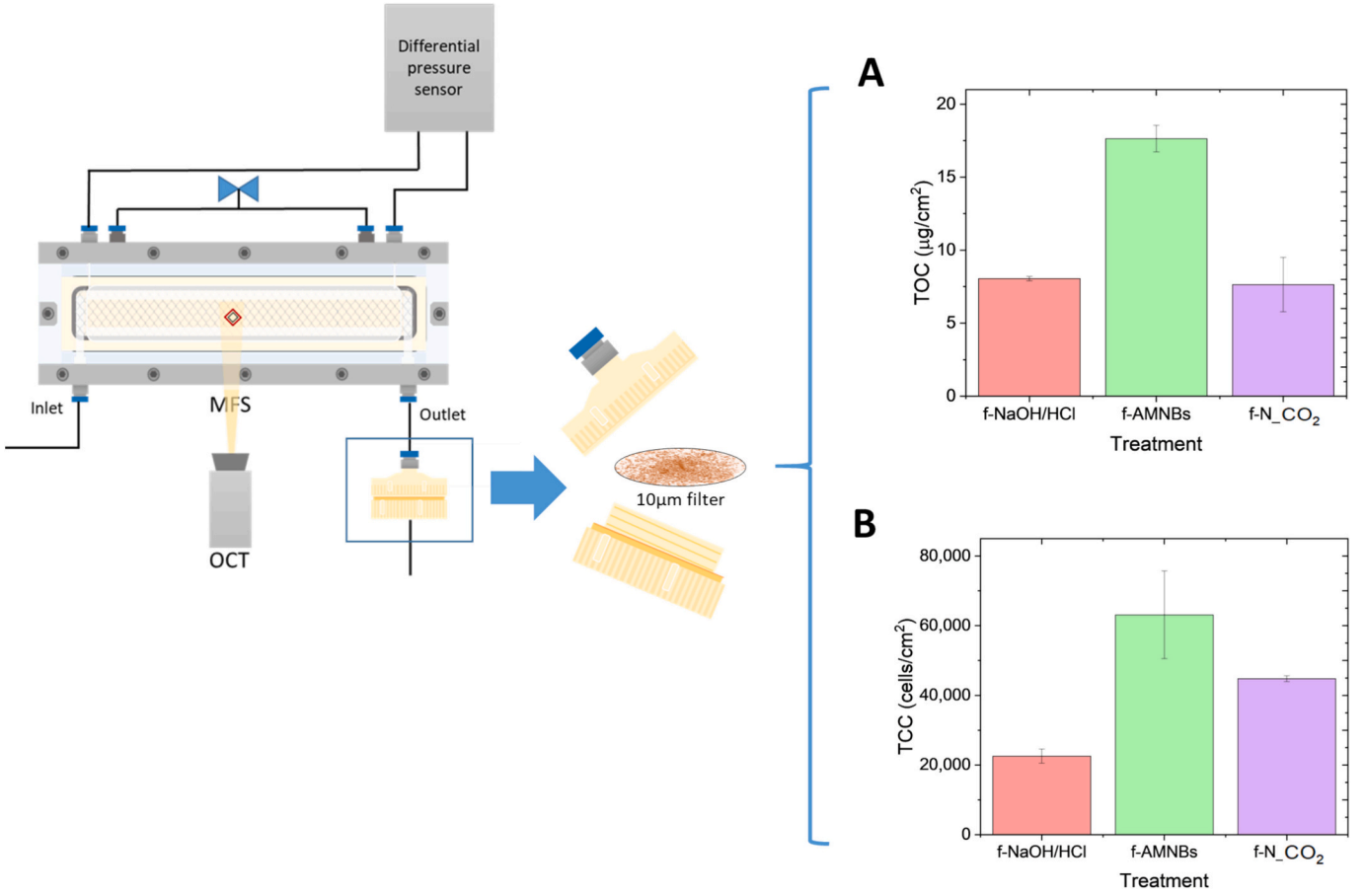

Fig. 6. Biomass autopsy for filter placed at MFS outlet during cleaning in place (CIP) quantified as total organic carbon (TOC) and total cell count (TCC) for seawater MFS experiments.

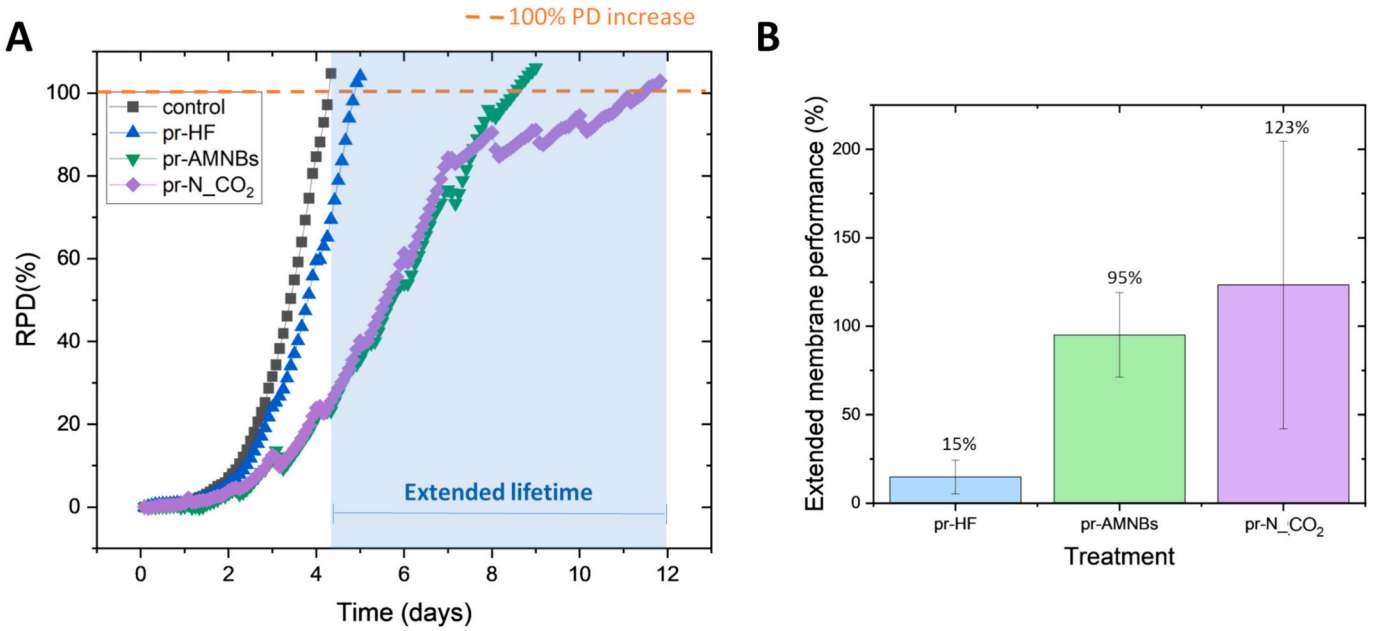

Fig. 7. A. Relative pressure drop (RPD) development in time from the start of nutrient dosing as day 0 for tap water preventive experiments during daily treatments and B) Average membrane performance duration before reaching a 100 % pressure drop (PD) increase per preventive treatment compared to the no treatment control.

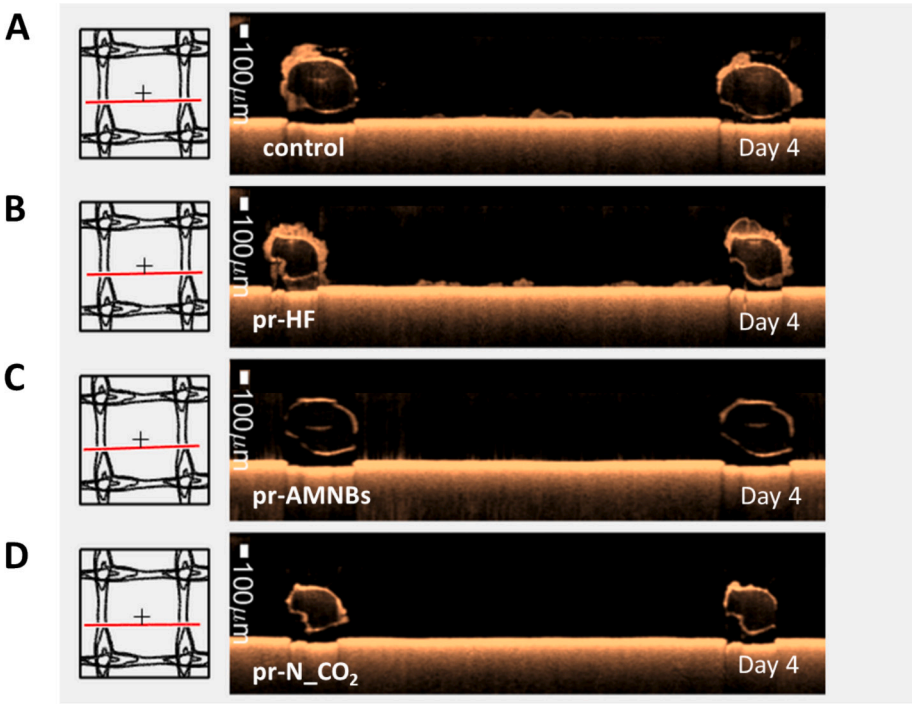

Fig. 8. Optical coherence tomography (OTC) images at day 4 for no preventive treatment (control), preventive hydraulic flushing (pr_HF), c) preventive air micro-nanobubbles treatment (pr_AMNBs), d) preventive pulsating Nucleated CO_2 bubbles generated at 1 bar (pr_CO_2).

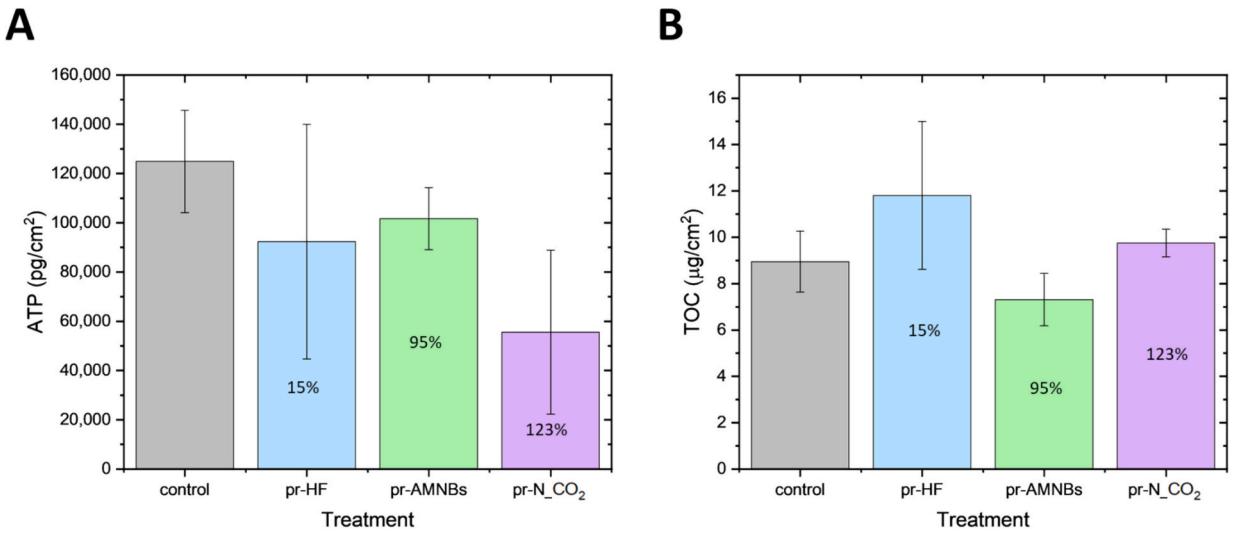

Fig. 9. Membrane biomass values quantified including extended membrane performance via A) adenosine triphosphate (ATP) and B) total organic carbon (TOC) for daily preventive treatments.

system as closely as possible with the membrane fouling simulators (MFS). Pressure drop was implemented as the main biofilm growth monitoring parameter as is used as such by standard industry practices [43].

4.1. MNBs enhanced biofilm detachment in seawater CIP

CIP treatments were performed once MFS reached a 100 % pressure drop increase and their cleaning efficiency was measured in terms of pressure drop decrease after treatment, as presented in Fig. 2. The majority of the growth was perceived around the feed spacer with minimal growth in the membrane surface in agreement with previous reports [46] and this growth occurred at a similar rate for both seawater and tap water environments since the biodegradable nutrient content was the same [49]. For the tap water, CIP cleaning efficiencies for the MNBs treatments (AMNBs & N_CO_2) and the chemical cleaning (NaOH/HCl) were within the 50 %–54 % range which is in agreement with previous reports of similar ~50 % cleaning efficiency for NaOH/HCl CIP utilizing lab scale tapwater MFS setups [47,50]. Surprisingly, all cleaning efficiencies increased for the seawater experiments. This fact could be attributed to the structural differences observed for seawater biofilms (see OCT images in Fig. 3), which may allow for better inactivation and detachment. It has been reported that microbial communities and diversity play an important role in the observed structural differences within seawater biofilms, accounting for an overall higher diversity of microbial taxa in comparison to tapwater biofilms [51,52]. In addition,

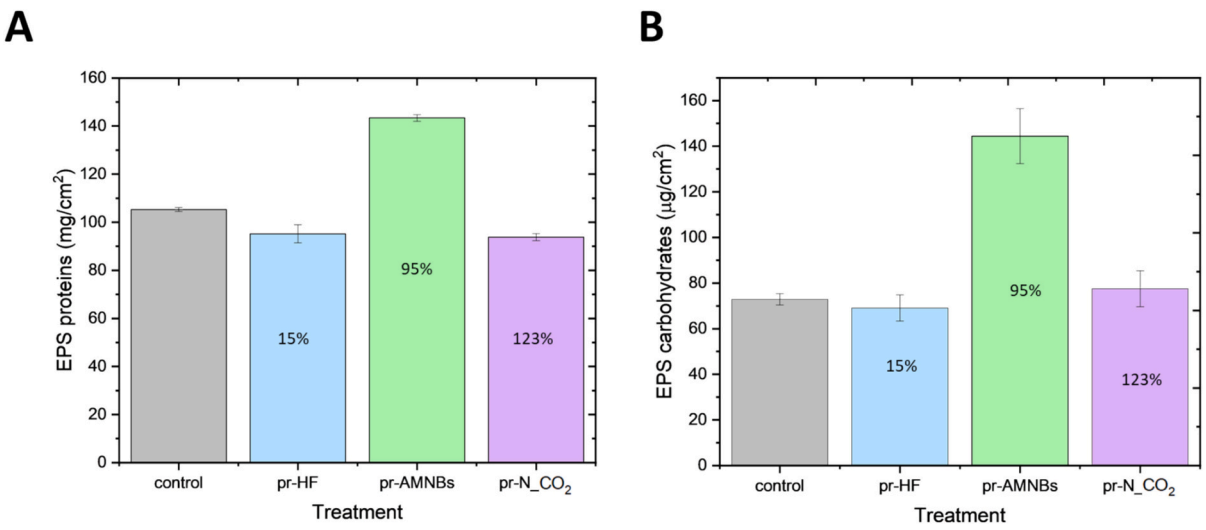

Fig. 10. Extracellular polymeric substances (EPS) quantification once a 100 % pressure drop increase was reached including extended membrane performance for A) total protein content and B) total carbohydrate content.

the lack of permeation on the seawater MFSs may have inhibited the growth of the seawater biofilm in the membrane due to a lack of nutrient attachment onto the membrane surface [53]. Nucleated CO_2 bubbles presented a higher cleaning efficiency at 71 % than the conventional chemical control with 63 %. This could entail that the additional shear force provided by the Nucleated CO_2 bubbles could have increased their detachment potential. It is important to acknowledge that the slight acidity of the solution (pH 3.9) may contribute to biofilm inactivation and removal. However, this effect is likely minimal, as previous studies have demonstrated that pH alone does not significantly influence the cleaning efficiency of organic fouling [30].

Furthermore, the presence of ions has no significant effect on MNB number and distribution [54]. Instead, they have been reported to enhance the stability of bulk MNBs [55 – 57] hence possibly enhancing the additional shear stress of MNBs into the biofilm at seawater environments.

AMNBs have only been previously evaluated for CIP treatment durations of an hour or longer [18,19,36,58]. Therefore, the major removal observation after 30 s presented in Supplementary Fig. 2 could lead to future shorter and more energy-efficient treatments. For the Nucleated CO_2 bubbles constant short pulsating treatments have been previously evaluated for synthetic fouling with promising cleaning efficiencies [34,59], which aligns with the fact that the major removal event was perceived within the first 15 s of exposure to the treatment.

Membrane autopsies occurred after the CIP procedures, for which a biomass reduction was noticeable for all of the evaluated treatments. The tap water hydraulic flush control accounted for high ATP values in comparison to the evaluated MNBs treatments. However, this difference was less noticeable for the TOC values, indicating a biomass inactivation property as the MNBs burst near the biofilm layer [18,19,60]. In agreement with previously discussed RPD and OCT image results, ATP and TOC values confirmed the better biomass removal efficiency under seawater conditions, with the Nucleated CO_2 bubbles accounting for values in a closer range of the chemical cleaning control. It is worth noting that ATP concentrations were overall lower for seawater experiments, which can be explained by an interference effect of the seawater ions [61].

Furthermore, autopsies of the filters used to collect the biomass coming out with the cross-flow water during seawater CIP treatments showed either similar or higher detached biomass values from the treated membranes than the chemical cleaning control. With AMNBs accounting for the highest overall biomass, this could be attributed to a better biomass integrity conservation by the neutral pH of the AMNBs solution.

Biomass inactivation and removal seemed more effective for the more complex and diverse microbial population environment of pre-treated seawater than dechlorinated tapwater. This would be highly beneficial for future applications in the water desalination industries if future pilot plant studies corroborate these results.

4.2. *Daily MNB treatments delayed biofouling and system performance decline*

Previous research regarding MNBs as preventive biofouling strategies has shown a significant delay in permeate flux and salt passage decline for 11 h with 2 min of AMNB treatments every 30 min and dosing with synthetic organic foulants [38]. Nevertheless, no long-term study on biofouling MNB prevention with less frequent treatments (i.e. daily) can be found in the current literature.

The daily MNB preventive treatments evaluated in this present article showed a significant delay in the system's performance decline measured in terms of pressure drop (PD) increase (100 %). This was perceived as an extension of the membrane performance of 123 % (5.1 days) for the Nucleated CO_2 bubbles experiments, 95 % (4 days) for the AMNBs, and 15 % (0.6 days) for the hydraulic flushing treatments compared to the control. Since the controls had a duration of 4.2 days, both MNB preventive treatments were able to double the system operation time to a certain extent. The Nucleated CO_2 bubbles preventive treatments showed a higher efficiency by 28 % (1.1 days) than AMNBs. This is consistent with the Nucleated CO_2 bubbles CIPs autopsy results, accounting for lower biomass amount.

Membrane autopsy took place once each MFS system reached a 100 % pressure drop (PD), and no preventive treatment was performed before the membrane autopsy. In agreement with the PD performance analysis ATP and TCC values were lower for the Nucleated CO_2 bubbles preventive treatments. However, TOC analysis resulted in AMNBs having the lowest value. Similarly, OCT images taken before preventive treatments at the growth monitoring point of 4 days (Fig. 7) show the least amount of growth for the AMNBs preventive treatments, even though the average RPD values at day 4 are roughly the same.

Interestingly, the MNB preventive treatments accounted for higher EPS carbohydrate and protein values than the controls, especially in the case of AMNBs. This can be explained by the longevity of the AMNBs treated membranes and their continuous exposure to 10 min of active AMNBs flush, which might have been enough time to negatively impact the biomass but not the sturdier EPS layer. Additionally, it has been

reported that EPS production increases under high shear stress by flow velocity [62], an effect that can be also attributed to the additional turbulence that MNBs repulsion forces generate in their liquid environment [36]. Similarly, AMNBs burst within the liquid solution could have introduced dissolved oxygen to the system. Dissolved oxygen has been previously reported to enhance EPS production, especially for carbohydrates [63]. This effect was not perceived by the Nucleated CO_2 bubbles due to the higher effectivity of pulsating treatments in comparison to a continuous flux [34], and the shorter treatment times. Therefore, the exposure to the Nucleated CO_2 bubbles intervals during 9 days may have resulted in lower biomass and slightly higher EPS growth.

While the laboratory-scale experiments conducted in this present study provide valuable insights into the effectiveness of air micro-nano bubbles (AMNBs) and nucleated CO_2 bubbles (N_CO_2) for biofilm removal and prevention, pilot plant testing remains a critical next step in assessing the long-term feasibility of these technologies for real SWRO systems. Pilot-scale evaluations would allow for a more comprehensive understanding of system performance under operational conditions, including the influence of varying feedwater compositions, hydrodynamic forces, and membrane module configurations. Additionally, testing at this scale would provide a better assessment of energy requirements, cleaning frequency, and overall operational costs, which are essential factors for large-scale implementation. Furthermore, an economic feasibility assessment should be integrated into pilot-scale studies to evaluate the cost-effectiveness of these cleaning strategies compared to conventional chemical cleaning, considering factors such as operational savings, energy consumption, and system longevity. Such an analysis will be crucial in determining the practical and financial viability of bubble-based cleaning technologies for full-scale applications. The promising results observed in this study, particularly the extended membrane lifespan and enhanced biofilm removal efficiencies, indicate the potential for significant operational benefits. However, pilot plant studies and economic assessments are necessary to validate these findings and optimize the application of bubble-based cleaning strategies to ensure their practical viability in full-scale desalination plants.

5. Conclusions

The present study evaluated the effectiveness of air-filled micro-nano bubbles (AMNBs) and saturated CO_2 nucleated bubbles (N_CO_2) as curative CIP and preventive strategies for biofouling cleaning and control. Feed channel pressure drop was the parameter used to monitor the developed biofilm impact on system performance and evaluate the efficiency of each cleaning treatment on the system performance restoration. Biofilm was analyzed once the feed channel pressure drop reached a 100 % increase, corresponding to 10–15 % over the full installation in agreement with industry standards. The performed experiments showed:

- Both air-filled and saturated CO_2 nucleated bubbles were as effective as conventional chemical cleaning in terms of pressure drop recovery. With the nucleated CO_2 bubbles surpassing the conventional chemical cleaning control in a seawater environment.
- Optical coherence tomography images before and after cleaning in place showed a clear biofilm reduction for all micro-nano bubble and nucleated CO_2 bubble treatments.
- Membrane autopsy results for micro-nano bubble and nucleated CO_2 bubble cleaning in place experiments showed lower overall biomass (ATP and TOC) in comparison with the hydraulic flush physical control.
- Daily preventive micro-nano bubble and nucleated CO_2 bubble treatments extended the performance of the membrane in terms of pressure drop increase by double. With the confirmation of optical coherence tomography images with minimal growth in comparison with the HF treatment and the control.
- Membrane autopsy results for preventive micro-nano bubble studies accounted for lower adenosine triphosphate and total organic carbon values than the physical cleaning control, but higher extracellular polymeric substances.

Overall, MNBs and nucleated CO_2 bubbles showed potential as effective curative and preventive strategies for biofouling control in comparison to conventional chemical and physical cleaning control. This effectivity was enhanced for seawater environments. With the additional advantage of lower treatment times and a lesser environmental footprint. Further studies are needed to confirm the cleaning efficiencies of this present study at a pilot scale and the economic feasibility of these promising technologies.

CRediT authorship contribution statement

Damaris S. Alvarez Sosa: Investigation, Data curation, Conceptualization, Methodology, Formal analysis, Writing – original draft, Software, Visualization. **Alla Alpatova:** Conceptualization, Methodology, Resources. **Doskhan Ybyraiymkul:** Conceptualization, Methodology, Resources. **Kim Choon Ng:** Supervision. **Noreddine Ghaffour:** Supervision. **Johannes S. Vrouwenvelder:** Supervision, Conceptualization, Funding acquisition. **Nadia Farhat:** Project administration, Conceptualization, Writing – review & editing, Funding acquisition, Validation.

Declaration of competing interest

The authors declare that they have no known competing financial interests or personal relationships that could have appeared to influence the work reported in this paper.

Acknowledgments

The research reported in this publication was supported by funding from King Abdullah University of Science and Technology (KAUST) under BAS/1/1401-01-01.

Appendix A. Supplementary data

Supplementary data to this article can be found online at https://doi.org/10.1016/j.desal.2025.118865.

Data availability

Data will be made available on request.

References

[1] N. Ghaffour, S. Soukane, J.G. Lee, Y. Kim, A. Alpatova, Membrane distillation hybrids for water production and energy efficiency enhancement: a critical review, Appl. Energy 254, no. February (2019) 113698, https://doi.org/10.1016/j.apenergy.2019.113698.
[2] S.F.E. Boerlage, M.D. Kennedy, M.P. Aniye, E.M. Abogrean, G. Galjaard, J. C. Schippers, Monitoring particulate fouling in membrane systems, Water Supply 17 (1) (1999) 213–224.
[3] J. Rolf, T. Cao, X. Huang, C. Boo, Q. Li, M. Elimelech, Inorganic scaling in membrane desalination: models, mechanisms, and characterization methods, Environ. Sci. Technol. 56 (12) (2022) 7484–7511, https://doi.org/10.1021/acs.est.2c01858.
[4] G. Amy, Fundamental understanding of organic matter fouling of membranes, Desalination 231 (1–3) (2008) 44–51, https://doi.org/10.1016/j.desal.2007.11.037.
[5] H.S. Vrouwenvelder, J.A.M. Van Paassen, H.C. Folmer, J.A.M.H. Hofman, M. M. Nederlof, D. Van Der Kooij, Biofouling of membranes for drinking water production, Desalination 118 (1–3) (1998) 157–166, https://doi.org/10.1016/S0011-9164(98)00116-7.
[6] J. Vrouwenvelder, J. Kruithof, Biofouling of Spiral Wound Membrane Systems, IWA Publishing, 2019.
[7] J.C. Te Lin, D.J. Lee, C. Huang, Membrane fouling mitigation: membrane cleaning, Sep. Sci. Technol. 45 (7) (2010) 858–872, https://doi.org/10.1080/01496391003666940.

[8] M. El Batouti, N.F. Alharby, M.M. Elewa, Review of New Approaches for Fouling Mitigation in Membrane Separation Processes in Water Treatment Applications, 2022.

[9] J. Huang, J. Luo, X. Chen, S. Feng, Y. Wan, How Do Chemical Cleaning Agents Act on Polyamide Nano fi ltration Membrane and Fouling Layer?, 2020, https://doi.org/10.1021/acs.iecr.0c03365.

[10] R. Terán Hilares, I. Singh, K. Tejada Meza, G.J. Colina Andrade, D.A. Pacheco Tanaka, Alternative methods for cleaning membranes in water and wastewater treatment, Water Environ. Res. 94 (4) (2022) 1–20, https://doi.org/10.1002/wer.10708.

[11] G. Trägårdh, Membrane cleaning, Desalination 71 (3) (1989) 325–335, https://doi.org/10.1016/0011-9164(89)85033-7.

[12] W. Cai, Y. Liu, Enhanced membrane biofouling potential by on-line chemical cleaning in membrane bioreactor, J. Memb. Sci. 511 (2016) 84–91, https://doi.org/10.1016/j.memsci.2016.03.039.

[13] N. AlSawaftah, W. Abuwatfa, N. Darwish, G.A. Husseini, A review on membrane biofouling: prediction, characterization, and mitigation, Membranes (Basel). 12 (12) (2022), https://doi.org/10.3390/membranes12121271.

[14] S. Haris, X. Qiu, H. Klammler, M.M.A. Mohamed, The use of micro-nano bubbles in groundwater remediation: a comprehensive review, Groundw. Sustain. Dev. 11, no. March (2020) 100463, https://doi.org/10.1016/j.gsd.2020.100463.

[15] G.Z. Kyzas, A.C. Mitropoulos, From bubbles to nanobubbles, Nanomaterials 11 (10) (2021), https://doi.org/10.3390/nano11102592.

[16] E.D. Michailidi, G. Bomis, A. Varoutoglou, E.K. Efthimiadou, A.C. Mitropoulos, E. P. Favvas, Fundamentals and Applications of Nanobubbles 30, 2019, https://doi.org/10.1016/B978-0-12-814178-6.00004-2.

[17] A. Agarwal, W.J. Ng, Y. Liu, Principle and applications of microbubble and nanobubble technology for water treatment, Chemosphere 84 (9) (2011) 1175–1180, https://doi.org/10.1016/j.chemosphere.2011.05.054.

[18] A. Agarwal, H. Xu, W.J. Ng, Y. Liu, Biofilm detachment by self-collapsing air microbubbles: a potential chemical-free cleaning technology for membrane biofouling, J. Mater. Chem. 22 (5) (2012) 2203–2207, https://doi.org/10.1039/c1jm14439a.

[19] A. Agarwal, W.J. Ng, Y. Liu, Cleaning of biologically fouled membranes with self-collapsing microbubbles, Biofouling 29 (1) (2013) 69–76, https://doi.org/10.1080/08927014.2012.746319.

[20] S. Zhou, et al., Untapped potential: applying microbubble and nanobubble technology in water and wastewater treatment and ecological restoration, ACS ES T Eng. 2 (9) (2022) 1558–1573, https://doi.org/10.1021/acsestengg.2c00117.

[21] A.W. Foudas, R.I. Kosheleva, E.P. Favvas, M. Kostoglou, A.C. Mitropoulos, G. Z. Kyzas, Fundamentals and applications of nanobubbles: a review, Chem. Eng. Res. Des. 189 (2023) 64–86, https://doi.org/10.1016/j.cherd.2022.11.013.

[22] M. Lee, E.Y. Lee, D. Lee, B.J. Park, Stabilization and fabrication of microbubbles: applications for medical purposes and functional materials, Soft Matter 11 (11) (2015) 2067–2079, https://doi.org/10.1039/c5sm00113g.

[23] J. Rodríguez-Rodríguez, A. Sevilla, C. Martínez-Bazán, J.M. Gordillo, Generation of microbubbles with applications to industry and medicine, Annu. Rev. Fluid Mech. 47 (2015) 405–429, https://doi.org/10.1146/annurev-fluid-010814-014658.

[24] E.P. Favvas, G.Z. Kyzas, E.K. Efthimiadou, A.C. Mitropoulos, Bulk nanobubbles, generation methods and potential applications, Curr. Opin. Colloid Interface Sci. 54 (2021) 101455, https://doi.org/10.1016/j.cocis.2021.101455.

[25] Y. Wang, T. Wang, Preparation method and application of nanobubbles: a review, Coatings 13 (9) (2023), https://doi.org/10.3390/coatings13091510.

[26] T. Temesgen, T.T. Bui, M. Han, T. Il Kim, H. Park, Micro and nanobubble technologies as a new horizon for water-treatment techniques: a review, Adv. Colloid Interface Sci. 246 (June) (2017) 40–51, https://doi.org/10.1016/j.cis.2017.06.011.

[27] C. Counil, E. Abenojar, R. Perera, A.A. Exner, Extrusion: a new method for rapid formulation of high-yield, monodisperse nanobubbles, Small 18 (24) (2022) 1–11, https://doi.org/10.1002/smll.202200810.

[28] S. Nazari, et al., Study of effective parameters on generating submicron (nano)-bubbles using the hydrodynamic cavitation, Physicochem. Probl. Miner. Process. 56 (5) (2020) 884–904, https://doi.org/10.37190/PPMP/126628.

[29] H. Syaeful Alam, P. Sutikno, T.A.F. Soelaiman, A.T. Sugiarto, Population balance modeling and multi-response optimization of a swirling-flow nanobubble generator, Chem. Eng. Technol. 45 (6) (2022) 1058–1166, https://doi.org/10.1002/ceat.202100360.

[30] H. Alnajjar, A. Tabatabai, A. Alpatova, T. Leiknes, N. Ghaffour, Organic fouling control in reverse osmosis (RO) by effective membrane cleaning using saturated CO_2 solution, Sep. Purif. Technol. 264 (August 2020) (2021) 118410, https://doi.org/10.1016/j.seppur.2021.118410.

[31] I.S. Ngene, et al., CO_2 nucleation in membrane spacer channels remove biofilms and fouling deposits, Ind. Eng. Chem. Res. 49 (20) (2010) 10034–10039, https://doi.org/10.1021/ie1011245.

[32] M.A. Al-Ghamdi, A. Alhadidi, N. Ghaffour, Membrane backwash cleaning using CO_2 nucleation, Water Res. 165 (2019) 114985, https://doi.org/10.1016/j.watres.2019.114985.

[33] A. Alpatova, A. Qamar, M. Al-Ghamdi, J.G. Lee, N. Ghaffour, Effective membrane backwash with carbon dioxide under severe fouling and operation conditions, J. Memb. Sci. 611, no. May (2020) 118290, https://doi.org/10.1016/j.memsci.2020.118290.

[34] M.A. Al-Ghamdi, A. Alpatova, A. Alhadidi, N. Ghaffour, Pulsating CO_2 nucleation radically improves the efficiency of membrane backwash, Desalination 520, no. May (2021) 115331, https://doi.org/10.1016/j.desal.2021.115331.

[35] A. Ghadimkhani, W. Zhang, T. Marhaba, Ceramic membrane defouling (cleaning) by air nano bubbles, Chemosphere 146 (2016) 379–384, https://doi.org/10.1016/j.chemosphere.2015.12.023.

[36] H.N.P. Dayarathne, J. Choi, A. Jang, Enhancement of cleaning-in-place (CIP) of a reverse osmosis desalination process with air micro-nano bubbles, Desalination 422 (August) (2017) 1–4, https://doi.org/10.1016/j.desal.2017.08.002.

[37] A. Rezvani Mahmouee, S.F. Saghravani, B. Dahrazma, Application of micro–nano bubbles to improve the performance of reverse-osmosis membrane against the gypsum scaling, J. Environ. Eng. 148 (1) (2022) 1–11, https://doi.org/10.1061/(asce)ee.1943-7870.0001935.

[38] A. Rezvani Mahmouee, S.F. Saghravani, B. Dahrazma, Evaluation of the anti-fouling effects of micro-nano bubbles on the performance of reverse osmosis membrane, J. Environ. Eng. 149 (4) (2023) 1–14, https://doi.org/10.1061/joeedu.eeeng-7072.

[39] M.U. Farid, J.A. Kharraz, C.H. Lee, J.K.H. Fang, S. St-Hilaire, A.K. An, Nanobubble-assisted scaling inhibition in membrane distillation for the treatment of high-salinity brine, Water Res. 209 (December 2021) (2022) 117954, https://doi.org/10.1016/j.watres.2021.117954.

[40] J.S. Vrouwenvelder, S.M. Bakker, L.P. Wessels, J.A.M. van Paassen, The Membrane Fouling Simulator as a new tool for biofouling control of spiral-wound membranes, Desalination 204, no. 1–3 SPEC. ISS (2007) 170–174, https://doi.org/10.1016/j.desal.2006.04.028.

[41] R. Alrowais, C. Qian, M. Burhan, D. Ybyraiymkul, M.W. Shahzad, K.C. Ng, A greener seawater desalination method by direct-contact spray evaporation and condensation (DCSEC): Experiments, Appl. Therm. Eng. 179, no. February (2020) 115629, https://doi.org/10.1016/j.applthermaleng.2020.115629.

[42] N. Siebdrath, N. Farhat, W. Ding, J. Kruithof, J.S. Vrouwenvelder, Impact of membrane biofouling in the sequential development of performance indicators: feed channel pressure drop, permeability, and salt rejection, J. Memb. Sci. 585 (May) (2019) 199–207, https://doi.org/10.1016/j.memsci.2019.05.043.

[43] DOW, *DOW FILMTEC*™ Membranes Cleaning Procedures for DOW FILMTEC FT30 Elements no. 609, 2022, pp. 1–7, doi: Form No. 609-23010-0211.

[44] H. Sanawar, L.H. Kim, N.M. Farhat, M.C.M. van Loosdrecht, J.S. Vrouwenvelder, Periodic chemical cleaning with urea: disintegration of biofilms and reduction of key biofilm-forming bacteria from reverse osmosis membranes, Water Res. X, vol. 13, no. August (2021) 100117, https://doi.org/10.1016/j.wroa.2021.100117.

[45] D. Hansen, D. Benner, M. Hilgenhöner, T. Leisebein, A. Brauksiepe, W. Popp, ATP measurement as method to monitor the quality of reprocessing flexible endoscopes, Ger. Med. Sci. 2 (2004) p. Doc04. [Online]. Available: http://www.ncbi.nlm.nih.gov/pubmed/19675687%0Ahttp://www.pubmedcentral.nih.gov/articlerender.fcgi?artid=PMC2703208.

[46] H. Liu, H.H.P. Fang, Extraction of extracellular polymeric substances (EPS) of sludges, J. Biotechnol. 95 (3) (2002) 249–256, https://doi.org/10.1016/S0168-1656(02)00025-1.

[47] L. Neu, C.R. Proctor, J.C. Walser, F. Hammes, Small-scale heterogeneity in drinking water biofilms, Front. Microbiol. 10, no. OCT (2019) 1–14, https://doi.org/10.3389/fmicb.2019.02446.

[48] F.A. Hammes, T. Egli, New method for assimilable organic carbon determination using flow-cytometric enumeration and a natural microbial consortium as inoculum, Environ. Sci. Technol. 39 (9) (2005) 3289–3294, https://doi.org/10.1021/es048277c.

[49] N. Farhat, F. Hammes, E. Prest, J. Vrouwenvelder, A uniform bacterial growth potential assay for different water types, Water Res. 142 (2018) 227–235, https://doi.org/10.1016/j.watres.2018.06.010.

[50] M. Jafari, A. D, J. Zlopasa, E.R. Cornelissen, J.S. Vrouwenvelder, A comparison between chemical cleaning efficiency in lab-scale and full-scale reverse osmosis membranes : Role of extracellular polymeric substances (EPS), J. Memb. Sci. 609, no. May (2020) 118189, https://doi.org/10.1016/j.memsci.2020.118189.

[51] J. Zhang, et al., Impact of blended tap water and desalinated seawater on biofilm stability, Desalin. Water Treat. 52 (31–33) (2014) 5806–5811, https://doi.org/10.1080/19443994.2013.816870.

[52] M. Podar, et al., Journal of Membrane Science Letters Microbial diversity analysis of two full-scale seawater desalination treatment trains provides insights into detrimental biofilm formation, J. Membr. Sci. Lett. 1 (1) (2021) 100001, https://doi.org/10.1016/j.memlet.2021.100001.

[53] L. Javier, L. Pulido-beltran, J.S. Vrouwenvelder, Permeation Increases Biofilm Development in Nanofiltration Membranes Operated with Varying Feed Water Phosphorous Concentrations, 2022.

[54] K. Zhou, V. Maugard, W. Zhang, J. Zhou, X. Zhang, Effects of Gas Type, Oil, Salts and Detergent on Formation and Stability of Air and Carbon Dioxide Bubbles Produced by Using a Nanobubble Generator, 2023.

[55] B. Park, S. Yoon, Y. Choi, J. Jang, S. Park, J. Choi, Stability of Engineered Micro or Nanobubbles for Biomedical Applications, 2020.

[56] S.M. Montazeri, N. Kalogerakis, G. Kolliopoulos, Effect of chemical species and temperature on the stability of air nanobubbles, Sci. Rep. (2023) 1–15, https://doi.org/10.1038/s41598-023-43803-6.

[57] N. Nirmalkar, A.W. Pacek, M. Barigou, Interpreting the interfacial and colloidal stability of bulk nanobubbles, Soft Matter 14 (47) (2018) 9643–9656, https://doi.org/10.1039/c8sm01949e.

[58] M.H.C. Harun, W.B. Zimmerman, Membrane defouling using microbubbles generated by fluidic oscillation, Water Sci. Technol. Water Supply 19 (1) (2019) 97–106, https://doi.org/10.2166/ws.2018.056.

[59] Kim, S. Li, N. Ghaffour, Evaluation of different cleaning strategies for different types of forward osmosis membrane fouling and scaling, J. Memb. Sci. 596 (November 2019) (2020) 117731, https://doi.org/10.1016/j.memsci.2019.117731.

[60] J. Zevnik, D. Stopar, Water Treatment by Cavitation: Understanding it at a Single Bubble - Bacterial Cell Level vol. 236, 2023, https://doi.org/10.1016/j.watres.2023.119956 no. December 2022.
[61] A. Abushaban, et al., Direct measurement of atp in seawater and application of ATP to monitor bacterial growth potential in SWRO pre-treatment systems, Desalin. Water Treat. 99 (February 2018) (2017) 91–101, https://doi.org/10.5004/dwt.2017.21783.
[62] C. Wang, L. Miao, J. Hou, P. Wang, J. Qian, S. Dai, The effect of flow velocity on the distribution and composition of extracellular polymeric substances in biofilms and the detachment mechanism of biofilms, Water Sci. Technol. 69 (4) (2014) 825–832, https://doi.org/10.2166/wst.2013.785.
[63] F. Ahimou, M.J. Semmens, G. Haugstad, P.J. Novak, Effect of protein, polysaccharide, and oxygen concentration profiles on biofilm cohesiveness, Appl. Environ. Microbiol. 73 (9) (2007) 2905–2910, https://doi.org/10.1128/AEM.02420-06.